Rational Prediction of Single Metal Atom Supported on Two Dimensional Metal Diborides for Electrocatalytic N₂ Reduction Reaction with Integrated Descriptor

Lei Ge†¹, Weiwei Xu†¹, Chongyang Chen¹, Chao Tang¹, Lai Xu¹*, and Zhongfang Chen²*

¹Institute of Functional Nano & Soft Materials (FUNSOM), Jiangsu Key Laboratory for Carbon-Based Functional Materials & Devices, Soochow University Suzhou, 215123, China

²Department of Chemistry, Institute for Functional Nanomaterials, University of Puerto Rico, Rio Piedras Campus, San Juan, Puerto Rico 00931, United States

†Contributed equally to this work

AUTHOR INFORMATION

Corresponding Author

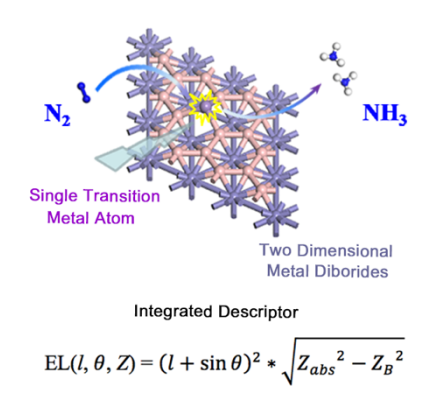
*E-mail: xulai15@suda.edu.cn (L. X.) ORCID: 0000-0003-2473-3359

*E-mail: zhongfangchen@gmail.com (Z. C.) ORCID: 0000-0002-1445-9184

ABSTRACT

Nitrogen reduction reaction (NRR) plays an important role in chemical industry, so it is significant to develop low-cost and efficient electrocatalysts for nitrogen fixation instead of traditional Haber-Bosch process. In this paper, the electrocatalytic performance of various single-atom doped on two dimensional metal diborides with B vacancy for N₂ reduction to ammonia is calculated and predicted. By screening numerous catalysts, we find that Ti@VB₂ is the most active catalyst for NRR, and the limiting potential of Ti@VB₂ for NRR is -0.61 V, which is far less than that of Ru (0001) step surface (-0.98 V). In addition, by comparing the change of free energy required for HER and NRR, it is proved that Ti@VB₂ has high NRR selectivity. Through high-throughput search and LASSO regression, an integrated descriptor combining the intrinsic properties of the single transition metal atom (TM) and the substrate (MB₂) is proposed, which can fit the relationship between intrinsic properties of catalysts and NRR activity well. Therefore, this study not only discovers a promising electrocatalyst for nitrogen fixation, but also provides a strategy for predicting the activity of catalysts.

TOC GRAPHIC



As one of the basic elements in amino acids, nitrogen plays a significant role in organisms.¹⁻⁵ Ammonia NH₃ is the most important product during the nitrogen reduction reaction and plays an important role in agriculture,⁶ chemical industry and energy field. In industry, the main process of N₂ fixation is still Haber-Bosch process. That is, the mixture of N₂ and H₂ is reduced to NH₃ with the assistance of catalysts at high temperature and high pressure. The whole reaction is

$$N_2(g) + 3H_2(g) \rightarrow 2NH_3(g)$$
 (1)

which is an exothermic reaction.⁷ During the Haber-Bosch process, due to the strong force of the $N\equiv N$ triple bond, it needs to consume lots of energy to activate and weaken the $N\equiv N$ bond and would produce much greenhouse gas, which is not friendly to the environment.⁸⁻¹⁰ Although researchers have improved the process for decades, the conversion efficiency of this reaction is only about 15%.¹¹ To solve this problem, many scientists turned the focus to the study of electrocatalytic nitrogen fixation. Compared with Haber-Bosch process, electrocatalytic reduction of N_2 has many advantages:1) the reaction can take place under the mild condition,^{12, 13} 2) the reaction rate, yield and selectivity are increased,¹⁴ 3) being beneficial to the environment. At present, researchers have studied, developed and utilized many NRR electrocatalysts, and most of them are metal-based catalysts, such as Ru, Pt, Ag, Mo, Rh and so on.¹⁵⁻¹⁹

Up to now, most studies have focused on design of new electrocatalysts to enhance the catalytic performance of the reaction, especially for the reduction of overpotential and improvement of Faraday efficiency. In recent years, many works have been reported on the experiments that single transition metal atoms were doped on different catalytic substrates, such as Fe-graphene,³ Mo-BN,⁴ Fe-TiO₂,²⁰ FeMoN₂,²¹ and TiN₄-graphene.²² The empty orbitals coexist with occupied d orbitals in transition metals, leading to their excellent catalytic performance. At the same time, they can accept the long-pair electrons of N₂, and supply

electrons to the antibonding orbital of N_2 to further activate $N \equiv N$ bond.²³ As reported before, the overpotential for N_2 reduction reaction on $Ti@N_4$ was found to be -0.69 eV by Choi et al. using theoretical studies.²² Therefore, the combination of transition metal single-atom and two-dimensional materials has significant catalytic effects on many catalytic reactions.

Recently, 2D boron-based materials has achieved great efficiency in catalytic fields. Ruatom-embedded on boron monolayer catalyst was proposed by Sun et al. for electrocatalytic nitrogen fixation at ambient condition, which shows good activity compared with Ru (0001) catalysts.²⁴ Moreover, to solve the problem of the electron deficiency of boron, Zhang et al. designed a new two dimensional single-layer of FeB₂ by theoretical calculation. It was also found that there is a Dirac point in FeB₂, which is mainly formed by hybridization of the d orbital of Fe and the p orbital of B.²⁵ This method has also been applied to design and simulate many other two-dimensional metal borides, such as MgB₂,²⁶ BeB₂²⁷ and TiB₂,²⁸ which exhibits superior electronic properties. Similarly, it would be feasible to synthesize single atom supported on two-dimensional metal-diborides (MB₂) easily in the experiment. However, studies about their performance in catalytic energy fields are very rare. In this work, the best catalytic activity of NRR (Ti@VB₂) was screened out from 45 single atom doped MB₂ structures by DFT calculations, and its limiting potential is -0.61 V.

However, specific guidelines are less sufficient during the process of designing high-performance catalysts in experiments. Therefore, how to extract a descriptor to characterize the catalytic activity of catalyst materials is of great significance. Most recently, the descriptors of some common electrocatalytic reactions were reported in theoretical calculations. For example, Calle-Vallejo et al. proposed the coordination number (\overline{CN}) as an effective descriptor for Pt-based catalysts to describe ORR activity.²⁹ Hammer et al. proved that d-band center (ε_d) can be

used as a descriptor for the chemisorption of CO₂ on metal surface.³⁰ For particular system like O-terminated MXenes, the number of electron O gains (N_e) was proposed to evaluate the HER performance.³¹ More recently, Jiang and his coworkers proved that the electronic dipole moment is a good descriptor to predict the interaction between the catalyst and surface molecule.³² Jiang and his coworkers also predicted surface-enhanced Raman spectroscopy (SERS) by using the random forest machine learning method.³³ Jung and his coworkers proposed about 20000 data set of alloy catalysts for CO₂ reduction by using the neural network machine learning method.³⁴ More significantly, with the rapid development of machine learning, some research achievements have been achieved in the prediction of materials.³⁵⁻³⁷ We can use known data about catalysts calculated by first principle calculations to predict the catalytic performance of more systems with machine learning techniques. After investigating the relationship between the free energy and one single variable for multiple linear fittings, we found that there is no linear relationship between the individual variables and the free energy, so we used the method of LASSO fitting (The Least Absolute Shrinkage and Selection Operator).³⁸ Through LASSO, a series of combined variables are sparse estimated, the variables are filtered, and the duplicate and invalid variables are deleted.³⁹ Finally, the LASSO fits the best regression and the descriptor called LASSO fitting expression is abbreviated as EL. This descriptor combines the intrinsic properties of the single atom (TM) and the substrate (MB₂). Therefore, combining with LASSO regression and high-throughput screening, we have predicted the NRR catalytic performance with different single atoms supported on a variety of metal diborides.

RESULTS AND DISSCUSION

We have selected several common structures from the fourth period in the periodic table of elements, which can form stable two-dimensional metal diborides with layered structures, they are ScB₂, TiB₂, VB₂ and FeB₂. In addition, MoB₂ layered compounds have been proven to have good catalytic activity in experiments and theoretical calculations,⁴⁰ and it has also been considered as a catalyst for N₂ reduction in this study. Therefore, five metal diborides with two-dimensional layered structure were selected in this work, namely ScB₂, TiB₂, VB₂, MoB₂ and FeB₂. Their optimized structures were shown in Figure 1. The metal atoms are located in the middle and lower part of the boron ring. This is consistent with the results reported recently,²⁵ which proved that FeB₂ can exist stably at temperatures below 1000 K.

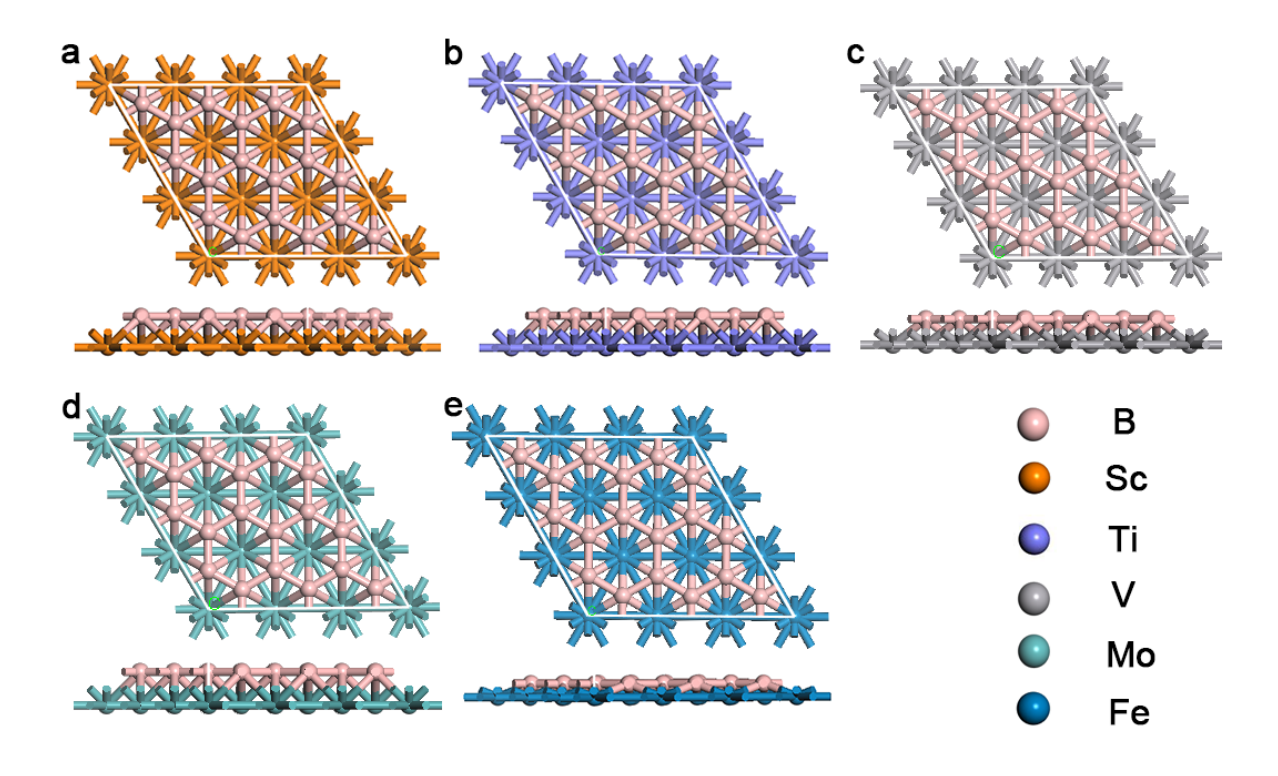


Figure 1. Optimized structures of two dimensional MB₂. (a) ScB₂, (b) TiB₂, (c) VB₂, (d) MoB₂, (e) FeB₂. The metal atoms are located in the middle and lower part of the boron ring.

Because the distance between B layer and metal layer is very close, which indicates that the interaction force between metal atom and B is stronger in single layer. In order to further study

the effect of the strong interaction between metal atom and B on the charge transfer of Sc, Ti, V, Mo, Fe and B, we calculated the Bader charge of these single layer structures. As shown in Table S1, each metal atom loses its electrons with positive charge, and B atom accepts electrons with negative charge. This phenomenon leads to the migration of electron to the boron layer framework, and is beneficial to the stability of these metal diborides. We also calculated the formation energy to confirm the interaction force between metal atom and B. We computed the formation energy by $\Delta E = (E(MB_2)-E(M)-2E(B))/3$, the formation energy is defined as the energy difference per unit cell between the monolayer MB2 and isolated atoms. E(MB2) means the energy of unit cell of monolayer MB₂, E(M) and E(B) represent the energy of metal atom M and B. Then we calculated the formation energy of each single layer, which is -0.23 eV/atom, -0.45 eV/atom, -0.42 eV/atom and -0.18 eV/atom for VB₂, TiB₂, ScB₂ and MoB₂ respectively. These results suggest that these monolayers are strongly bonded networks. About the structure of monolayer FeB₂, it was confirmed that the monolayer has strong interaction between metal atom Fe and B by calculating the cohesive energy.²⁵ Therefore, we can confirm that these five single layer structures have strong interaction between metal atom and B. In addition, the B layer is electron-rich, which is important in the reductive catalytic reaction. Recently, MoS₂ nanosheet with S vacancy was found that the S defect site can be used as a new active center for supporting and doping metal atoms. 41 Besides, Co@MoS2 and Mo@MoS2 were proven to be a promising NRR catalyst calculated by DFT calculations. 42, 43, 44 Therefore, in this work we studied the single transition metal atom supported on the B defective site of MB₂ single layer, which would be used for NRR. Nine common transition metals in the fourth period of the periodic table were selected as doped atoms at B defective site. Due to the magnetic and electronic properties of the d-orbital of the transition metal, we used the GGA + U calculation method for the adsorbed single metal

atom and the metal of the substrate.^{45, 46} The structure diagram of TM@MB₂ can be shown in Figure S1.

It is noteworthy that the adsorption of N₂ on the active center of catalysts is the first step in nitrogen fixation reaction and has a key role in the following hydrogenation reduction routes.⁴⁷ Therefore, two possible nitrogen adsorption configurations were considered in the calculations, i.e. side-on and end-on configurations (see Figure S2). In this calculation, we also consider the reaction site for doping metal atom in the metal layer or the B layer (see Figure S3). Finally, we proved that the transition metal doped in the B layer with the end-on adsorption configuration is more stable than the other adsorption configurations (detailed information is Figure S3).

It has been reported that the free energy change of NNH* formation from N_2 * hydrogenation (N_2 * + $H^+ \rightarrow N_2H^*$) in the electrocatalytic reduction of NRR by Nørskov and his coworkers, which is regarded as the judgment step to preliminarily judge the performance of the whole NRR pathway. Hence, before simulating the complete NRR routes on the single-atom catalysts, we should calculate the ΔG of NNH* formation in order to search for the most promising candidate for nitrogen electroreduction and the results were shown in Figure 2. It was known that the free energy change of NNH* formation from N_2 * hydrogenation (N_2 * + $H^+ \rightarrow N_2H^*$) on Ru (0001) stepped surface was about 0.98 eV, which is the lowest one among bulk metal catalysts and was provided as the reference (the black line shown in Figure 2). Our results showed that ScB_2 -based and TiB_2 -based single-atom catalysts exhibit the worst catalytic activity, and the change of free energy in the first step of hydrogenation are all larger than 0.98 eV. However, the system of $Ti@VB_2$ exhibits the best N_2 activation performance and the change of free energy in the first step for N_2 hydrogenation on $Ti@VB_2$ is only 0.61 eV, whose value is much lower than the value of the free energy change on Ru (0001) surface.

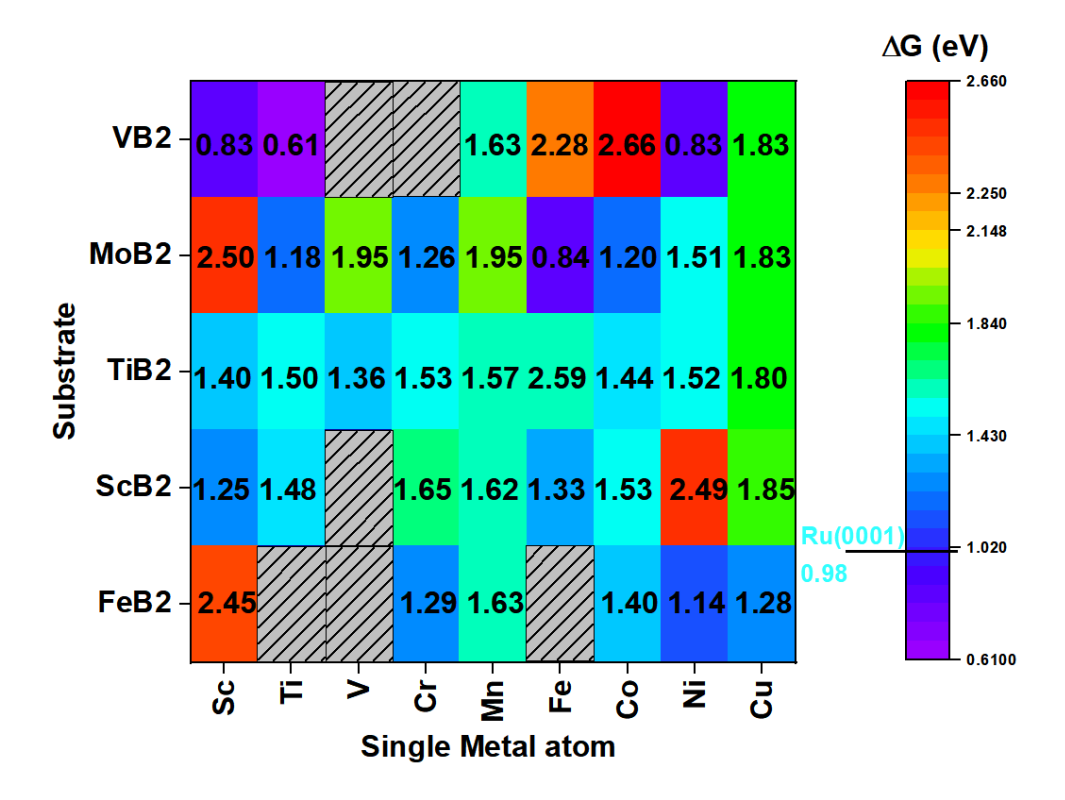


Figure 2. The change of free energy in the first step of N_2 hydrogenation reaction ($N_2* + H* \rightarrow N_2H*$) on various single metal atoms supported on two dimensional B-defective metal diborides, which is regarded as the judgment step of the whole NRR reaction. The maximum free energy change for NRR on the Ru (0001) stepped surface was provided as a reference. The values corresponding to various colors are shown on the right ruler.

Based on the change of free energy in the first step of hydrogenation, Ti@VB₂ has been proven to be the most promising candidate for NRR catalysis as shown in Figure 2. For further studying the catalytic performance of Ti@VB₂ for NRR, we simulated three possible NRR catalytic pathways on Ti single atom doped on VB₂, namely alternating mechanism, distal mechanism and enzymatic mechanism (as shown in Scheme S1).³ We optimized all the adsorption configurations in the reaction process according to the different paths mentioned above, and obtained the zero-point energy and the free energy by calculating the frequencies.

The corresponding structures of the three reaction routes and the paths of free energy change of reactions were shown in Figure 3a-3c. In the alternating route (see Figure 3a), hydrogenation takes place preferentially on alternating N each step to form NH₃, respectively. In the first step of hydrogenation, and the change of reaction free energy is 0.61 eV, showing a slightly upward slope. In the next steps, H⁺ continues to attack the intermediates until NH₃ is formed. Among these steps it can be found that from the second step, there is a downward energy change trend, which also makes the subsequent reaction easier. From Figure 3a we can find that N₂ hydrogenation to N₂H* is the rate-determining step of the whole reaction in the alternating pathway, with the highest $\Delta G = 0.61 \text{ eV}$.

In the routes of distal (see Figure 3b) and enzymatic (see Figure 3c) mechanisms, hydrogenation takes place alternately between the two N atoms. In the path of distal mechanism and enzymatic mechanism, the rate-determining step of free energy change in nitrogen fixation reaction is the same as that of alternating pathway, which occurs in the first step of N_2 hydrogenation, and $\Delta G = 0.61$ eV for distal mechanism, while $\Delta G = 1.07$ eV for the enzymatic mechanism due to different approach of N_2 adsorption.

Therefore, under the reversible hydrogen electrode (RHE), the limiting potential of Ti@VB₂ for NRR catalytic reaction is -0.61 V, that is, a potential of -0.61 V is needed to ensure that every step of NRR catalyzed by Ti@VB₂ can occur, and the distal and alternating mechanisms may both occur among three mechanisms. Compared with the reported NRR catalyzed by Ru (0001) surface, the limiting potential required by Ti@VB₂ is about half of the potential required by Ru (-0.98 V).⁴⁹ About the stability of VB₂, in the experiment, VB₂ bulk has been proven to have high thermal stability at 1410 K in air.⁵⁰ For two-dimensional VB₂, we performed AIMD simulations at different temperatures and phonon dispersion stability

calculations as shown in Figure S4 (detail information as shown in SI). Then we considered the stability of Ti@VB₂. We calculated the binding energy of Ti@VB₂ which is -1.26 eV, from the value of binding energy we can find that the doping structure of Ti@VB₂ is also stable. About the method of binding energy computation, we used the following formula, $E_{binding} = E_{Ti@VB2} - E_{VacancyVB2} - E_{Ti} \cdot E_{binding}$ represents the binding energy of Ti@VB₂, $E_{Ti@VB2}$ represents the energy of Ti@VB₂, $E_{Vacancy}$ represents the energy of VB₂ with B vacancy, and E_{Ti} represents the energy of single metal atom Ti.

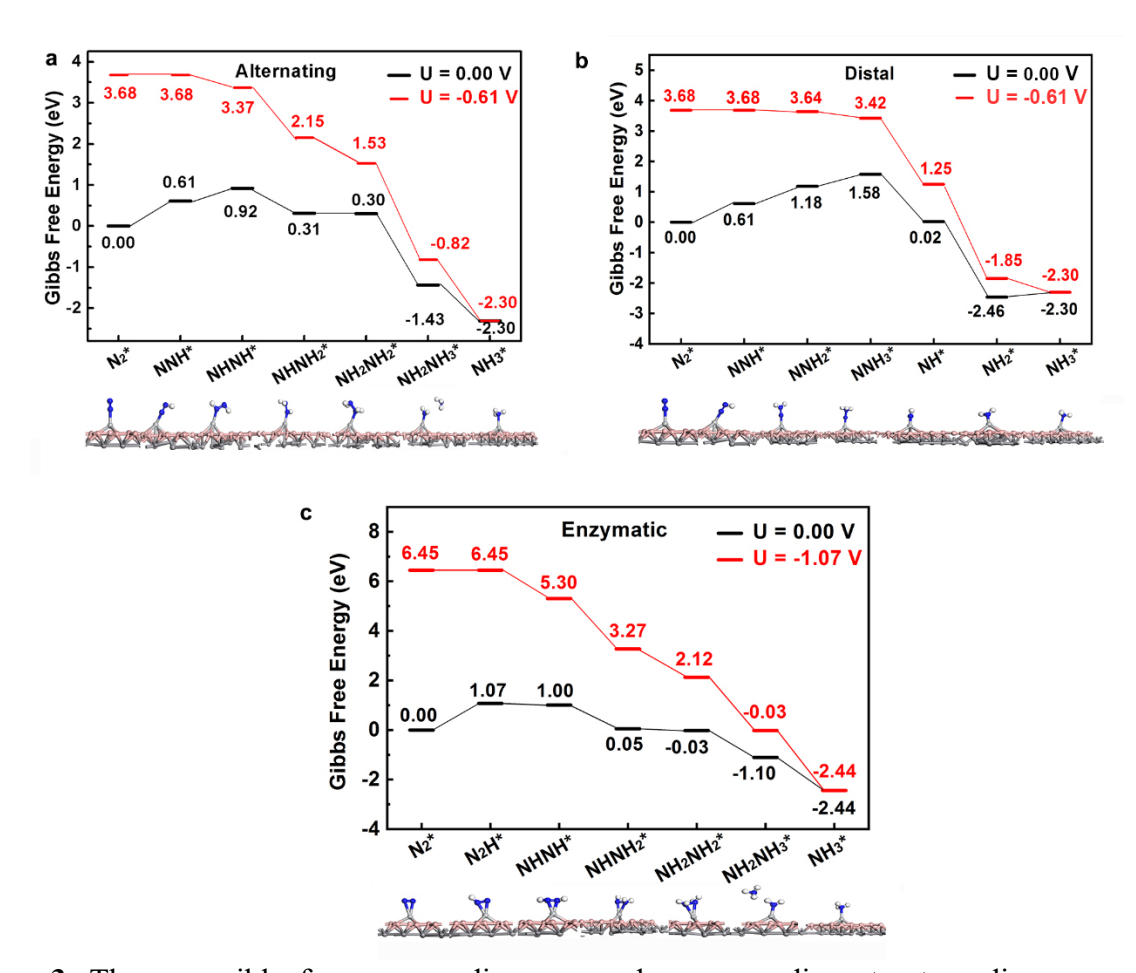


Figure 3. Three possible free energy diagrams and corresponding structure diagrams of N₂ reduction catalyzed by Ti@VB₂.

It is well known that HER is the main competitive reaction in electrocatalytic nitrogen fixation reaction, which seriously affects the efficiency of nitrogen reduction. Herein, we used the free energy change of the first step as the descriptor to judge the selectivity of HER and NRR on Ti@VB₂ catalyst as shown in Figure S5 (detailed information as shown in SI).

To further understand the catalytic performance of Ti@VB₂ catalyst, the Bader charges for all the intermediate states in the alternating route (shown in Figure S6a) and distal route (shown in Figure S6b) were calculated (detailed information as shown in SI). We analyzed the charge density difference of the end-on adsorption configuration of N_2 . As shown in Figure 4, it is obvious that charge depletion and accumulation take place between N_2 and Ti atom. Because of the existence of long pair electrons in N_2 , it would donate electrons when it binds to Ti atom. Meanwhile, Ti atom also gives electrons to the anti-bonding orbital of N_2 with the enhancement of the N-TM bond. This phenomenon is consistent with the 'acceptance-donation' process, 1,51,52 which will activate N_2 and make the breakage of $N\equiv N$ bond easier. These phenomena can be explained by the schematic diagram (Figure S7). 1,51

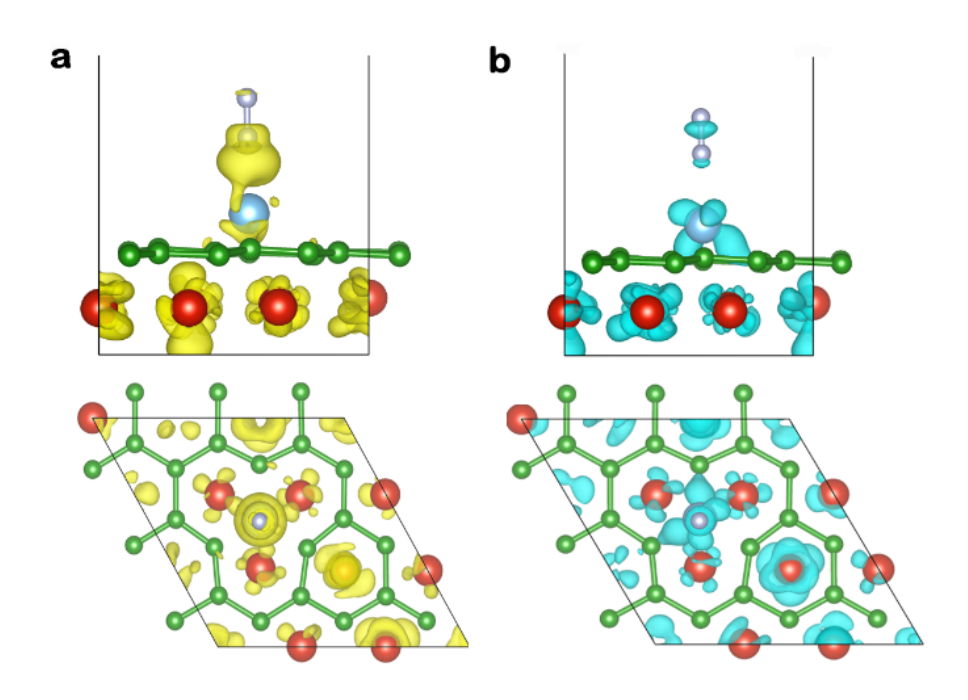


Figure 4. The main view (top) and the side view (bottom) of the charge density difference of N_2 adsorbed on $Ti@VB_2$, (a) the positive and (b) negative charges are shown in yellow and cyan.

Based on density functional theory, the catalytic performance of N₂ reduction reaction on five different metal diborides supported with nine different single atoms was studied, and we finally found that Ti@VB₂ has the highest NRR catalytic activity. In order to further study the relationship between catalysts and catalytic activity, we hope to extract a descriptor that can characterize the catalytic activity based on the data obtained, which will be beneficial to predict the catalytic activity of more similar systems. As reported before, we have known that the intrinsic properties, such as atomic composition, electronegativity, and valence electron numbers which can be derived from the periodic table, play a leading role in catalytic performance prediction.^{53, 54} In this work, the system we are studying is TM@MB₂, so we need to consider the properties of single metal atoms and the substrates comprehensively.

In this article, we used the atomic number, valence electron number, electronegativity, radius (Å), relative atomic mass, ionization potential-1st, ionization potential-2rd, electron affinity (eV) as the atomic intrinsic properties, and used the length of absorbed metal and the atom of N (Å), sine value of the angle between three atoms (the atom B, absorbed metal and the atom N) as the system intrinsic properties. Then we set these properties as the input, the ΔG for $N_2* + H^+ \rightarrow N_2H*$ as the output. In order to find the relationship between the energy and the intrinsic properties of catalysts, we want to find linear relationship to describe the intuitive relationship. There are many shrinkage methods such as ridge regression, and LASSO regression. LASSO regression (least absolute shrinkage and selection operator regression) can find descriptors and fit

the linear relationship for small data sets.³⁸ In this article, we chose the method of LASSO regression in MATLAB to fit the linear relationship.

From the descriptor mentioned above, we have known that the intrinsic properties of catalysts are of great significance on the activity of NRR. To predict the activity performance for more similar systems, we tried to use LASSO regression technology in Matlab to establish a suitable model.⁵⁵ The closer R² is to 1, the better the fitting effect. After entering these variables as mentioned before, we got the result of the descriptor, which is $EL(l, \theta, Z) = (l + \sin \theta)^2 * \sqrt{Z_{abs}^2 - Z_B^2}$, and l means the bond length of N_TM, $\sin \theta$ means the sin value of the angle TM_N_B (As for the selection of atom B, we chose the atom B closest to TM atom along the Y-axis in a spatial coordinate system), detailed structure information are shown in Figure 5. Z_{abs} means the atomic number of absorbed metal and Z_B means the atomic number of boron atom. From this descriptor, we find the relationship between the ΔG of $N_2*+ H^+ \rightarrow N_2H^*$ for these five systems and the intrinsic properties. We find that the relationship is y = 0.01x - 0.15, and R² is 0.81.

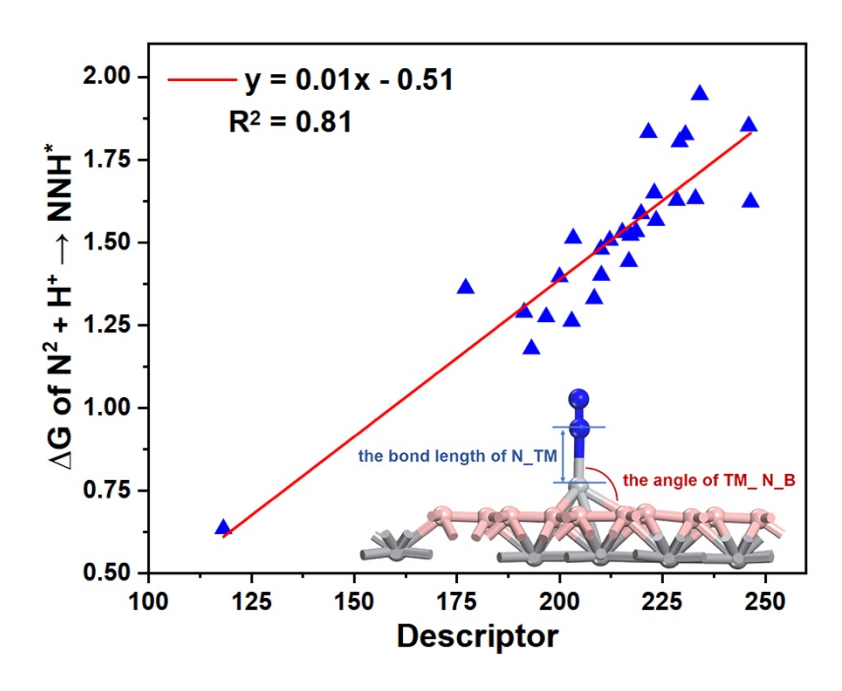


Figure 5. The relationship between the descriptor $EL(l, \theta, Z) = (l + \sin \theta)^2 * \sqrt{Z_{abs}}^2 - Z_B^2$ and ΔG of the reaction of $N_2*+H^+\rightarrow N_2H^*$.

SUMMARY AND CONCLUSIONS

In summary, we attempted to apply two-dimensional metal diborides for N₂ reduction catalysis. Various single-atom supported on different metal diborides was systematically studied for NRR electrocatalysis. The results of DFT calculations showed that Ti@VB₂ nanosheet has high NRR catalytic performance, and its Gibbs free energy change of rate-determining step is -0.61 V, which is lower than that of Ru (0001) stepped surface. Moreover, it was proved that Ti@VB₂ has better NRR selectivity than HER. In addition, an integrated descriptor EL(l, θ , Z) = $(l + \sin \theta)^2 * \sqrt{Z_{abs}^2 - Z_B^2}$ to describe the catalytic performance of single-atom supported on MB₂ was proposed by LASSO approach. Our study offers an efficient strategy for predicting the activity of catalysts for further screening of highly efficient catalysts.

AUTHOR INFORMATION

Notes

The authors declare no competing financial interests.

ACKNOWLEDGMENT

We acknowledge financial support from Natural Science Foundation of China (Grant No. 91961120), Innovative and Entrepreneurial Doctor (World-Famous Universities) in Jiangsu Province, and Talent in Demand in the city of Suzhou. This project is also funded by the Collaborative Innovation Center of Suzhou Nano Science & Technology, the Priority Academic Program Development of Jiangsu Higher Education Institutions (PAPD), the 111 Project, and

Joint International Research Laboratory of Carbon-Based Functional Materials and Devices. This work is also supported in USA by the National Science Foundation-Centers of Research Excellence in Science and Technology (NSF-CREST Center) for Innovation, Research and Education in Environmental Nanotechnology (CIRE2N) (Grant HRD-1736093). We thank Jinxing Gu and Shiru Lin for their insightful suggestions.

Supporting Information.

The following files are available free of charge.

Computed methods; The Bader charge of two-dimensional; the structure diagram; the adsorption energies of N₂; the phonon dispersion and AIMD; the selectivity of NRR versus HER; the Bader charges of Ti@VB₂ catalyst; schematic diagram of N₂ interacting with TM center. (PDF)

REFERENCES

- (1) Légaré, M.-A.; Bélanger-Chabot, G.; Dewhurst, R. D.; Welz, E.; Krummenacher, I.; Engels, B.; Braunschweig, H., Nitrogen Fixation and Reduction at Boron. *Science* **2018**, *359*, 896-900.
- (2) Li, H.; Shang, J.; Ai, Z. H.; Zhang, L. Z., Efficient Visible Light Nitrogen Fixation with BiOBr Nanosheets of Oxygen Vacancies on the Exposed {001} Facets. *Journal of the American Chemical Society* **2015**, *137*, 6393-6399.
- (3) Li, X. F.; Li, Q. K.; Cheng, J.; Liu, L. L.; Yan, Q.; Wu, Y. C.; Zhang, X. H.; Wang, Z. Y.; Qiu, Q.; Luo, Y., Conversion of Dinitrogen to Ammonia by FeN₃-Embedded Graphene. *Journal of the American Chemical Society* **2016**, *138*, 8706-8709.
- (4) Zhao, J. X.; Chen, Z. F., Single Mo Atom Supported on Defective Boron Nitride Monolayer as an Efficient Electrocatalyst for Nitrogen Fixation: A Computational Study. *Journal of the American Chemical Society* **2017**, *139*, 12480-12487.
- (5) Schlögl, R., Catalytic Synthesis of Ammonia—A "Never Ending Story"? *Angewandte Chemie International Edition* **2003**, *42*, 2004-2008.
- (6) Kitano, M.; Inoue, Y.; Yamazaki, Y.; Hayashi, F.; Kanbara, S.; Matsuishi, S.; Yokoyama, T.; Kim, S.-W.; Hara, M.; Hosono, H., Ammonia Synthesis Using a Stable Electride as an Electron Donor and Reversible Hydrogen Store. *Nature chemistry* **2012**, *4*, 934.
- (7) Haber, F., Neue Arbeitsweisen. *Naturwissenschaften* **1923**, *11*, 753-756.
- (8) Van der Ham, C. J. M.; Koper, M. T. M.; Hetterscheid, D. G. H., Challenges in reduction of dinitrogen by proton and electron transfer. *Chemical Society Reviews* **2014**, *43*, 5183-5191.

- (9) Jia, H. P.; Quadrelli, E. A., Mechanistic aspects of dinitrogen cleavage and hydrogenation to produce ammonia in catalysis and organometallic chemistry: relevance of metal hydride bonds and dihydrogen. *Chemical Society Reviews* **2014**, *43*, 547-564.
- (10) Kandemir, T.; Schuster, M. E.; Senyshyn, A.; Behrens, M.; Schlögl, R., The Haber–Bosch process revisited: On the real structure and stability of "ammonia iron" under working conditions. *Angewandte Chemie International Edition* **2013**, *52*, 12723-12726.
- (11) Foster, S. L.; Bakovic, S. I. P.; Duda, R. D.; Maheshwari, S.; Milton, R. D.; Minteer, S. D.; Janik, M. J.; Renner, J. N.; Greenlee, L. F., Catalysts for nitrogen reduction to ammonia. *Nature Catalysis* **2018**, *1*, 490-500.
- (12) Murakami, T.; Nishikiori, T.; Nohira, T.; Ito, Y., Electrolytic synthesis of ammonia in molten salts under atmospheric pressure. *Journal of the American Chemical Society* **2003**, *125*, 334-335.
- (13) Zhou, F.; Azofra, L. M.; Ali, M.; Kar, M.; Simonov, A. N.; McDonnell-Worth, C.; Sun, C.; Zhang, X.; MacFarlane, D. R., Electro-synthesis of ammonia from nitrogen at ambient temperature and pressure in ionic liquids. *Energy & Environmental Science* **2017**, *10*, 2516-2520.
- (14) Marnellos, G.; Stoukides, M., Ammonia synthesis at atmospheric pressure. *Science* **1998**, 282, 98-100.
- (15) Thompson, N. B.; Green, M. T.; Peters, J. C., Nitrogen fixation via a terminal Fe (IV) nitride. *Journal of the American Chemical Society* **2017**, *139*, 15312-15315.
- (16) Lehnert, N.; Peters, J. C., Preface for Small-Molecule Activation: From Biological Principles to Energy Applications. Part 2: Small Molecules Related to the Global Nitrogen Cycle. *Inorg Chem* **2015**, *54*, 9229-9233.
- (17) Rittle, J.; Peters, J. C., An Fe-N₂ Complex That Generates Hydrazine and Ammonia via Fe NNH₂: Demonstrating a Hybrid Distal-to-Alternating Pathway for N₂Reduction. *Journal of the American Chemical Society* **2016**, *138*, 4243-4248.
- (18) Del Castillo, T. J.; Thompson, N. B.; Suess, D. L.; Ung, G.; Peters, J. C., Evaluating molecular cobalt complexes for the conversion of N₂ to NH₃. *Inorg Chem* **2015**, *54*, 9256-9262.
- (19) Fajardo Jr, J.; Peters, J. C., Catalytic nitrogen-to-ammonia conversion by osmium and ruthenium complexes. *Journal of the American Chemical Society* **2017**, *139*, 16105-16108.
- (20) Zhao, W.; Zhang, J.; Zhu, X.; Zhang, M.; Tang, J.; Tan, M.; Wang, Y., Enhanced nitrogen photofixation on Fe-doped TiO2 with highly exposed (1 0 1) facets in the presence of ethanol as scavenger. *Applied Catalysis B: Environmental* **2014**, *144*, 468-477.
- (21) Li, Q.; He, L.; Sun, C.; Zhang, X., Computational study of MoN₂ monolayer as electrochemical catalysts for nitrogen reduction. *The Journal of Physical Chemistry C* **2017**, *121*, 27563-27568.
- (22) Choi, C.; Back, S.; Kim, N.-Y.; Lim, J.; Kim, Y.-H.; Jung, Y., Suppression of Hydrogen Evolution Reaction in Electrochemical N2 Reduction Using Single-Atom Catalysts: A Computational Guideline. *ACS Catalysis* **2018**, *8*, 7517-7525.
- (23) Legare, M. A.; Belanger-Chabot, G.; Dewhurst, R. D.; Welz, E.; Krummenacher, I.; Engels, B.; Braunschweig, H., Nitrogen fixation and reduction at boron. *Science* **2018**, *359*, 896-899.
- (24) Liu, C.; Li, Q.; Zhang, J.; Jin, Y.; MacFarlane, D. R.; Sun, C., Conversion of dinitrogen to ammonia on Ru atoms supported on boron sheets: a DFT study. *J Mater Chem A* **2019**, *7*, 4771-4776.

- (25) Zhang, H.; Li, Y.; Hou, J.; Du, A.; Chen, Z., Dirac State in the FeB₂ Monolayer with Graphene-Like Boron Sheet. *Nano Letters* **2016**, *16*, 6124-6129.
- (26) Tang, H.; Ismail-Beigi, S., Self-doping in boron sheets from first principles: A route to structural design of metal boride nanostructures. *Physical Review B* **2009**, *80*, 134113.
- (27) Zhang, P.; Crespi, V. H., Theory of B₂O and BeB₂ Nanotubes: New Semiconductors and Metals in One Dimension. *Physical review letters* **2002**, 89, 056403.
- (28) Zhang, L.; Wang, Z.; Du, S.; Gao, H.-J.; Liu, F., Prediction of a Dirac state in monolayer TiB₂. *Physical Review B* **2014**, *90*, 161402.
- (29) Calle-Vallejo, F.; Tymoczko, J.; Colic, V.; Vu, Q. H.; Pohl, M. D.; Morgenstern, K.; Loffreda, D.; Sautet, P.; Schuhmann, W.; Bandarenka, A. S., Finding Optimal Surface Sites on Heterogeneous Catalysts by Counting Nearest Neighbors. *Science* **2015**, *350*, 185-189.
- (30) Hammer, B.; Morikawa, Y.; Nørskov, J. K., CO Chemisorption at Metal Surfaces and Overlayers. *Physical review letters* **1996,** *76*, 2141.
- (31) Ling, C.; Shi, L.; Ouyang, Y.; Wang, J., Searching for Highly Active Catalysts for Hydrogen Evolution Reaction Based on O-terminated MXenes Through a Simple Descriptor. *Chemistry of Materials* **2016**, *28*, 9026-9032.
- (32) Wang, X.; Ye, S.; Hu, W.; Sharman, E.; Liu, R.; Liu, Y.; Luo, Y.; Jiang, J., Electric Dipole Descriptor for Machine Learning Prediction of Catalyst Surface–Molecular Adsorbate Interactions. *Journal of the American Chemical Society* **2020**, *142*, 7737-7743.
- (33) Hu, W.; Ye, S.; Zhang, Y.; Li, T.; Zhang, G.; Luo, Y.; Mukamel, S.; Jiang, J., Machine Learning Protocol for Surface-Enhanced Raman Spectroscopy. *The Journal of Physical Chemistry Letters* **2019**, *10*, 6026-6031.
- (34) Gu, G. H.; Noh, J.; Kim, S.; Back, S.; Ulissi, Z.; Jung, Y., Practical Deep-Learning Representation for Fast Heterogeneous Catalyst Screening. *The Journal of Physical Chemistry Letters* **2020**, *11*, 3185-3191.
- (35) Pilania, G.; Wang, C.; Jiang, X.; Rajasekaran, S.; Ramprasad, R., Accelerating materials property predictions using machine learning. *Scientific reports* **2013**, *3*, 2810.
- (36) Hautier, G.; Fischer, C. C.; Jain, A.; Mueller, T.; Ceder, G., Finding nature's missing ternary oxide compounds using machine learning and density functional theory. *Chemistry of Materials* **2010**, *22*, 3762-3767.
- (37) Rupp, M.; Tkatchenko, A.; Müller, K.-R.; Von Lilienfeld, O. A., Fast and accurate modeling of molecular atomization energies with machine learning. *Physical review letters* **2012**, *108*, 058301.
- (38) Lee, C.-Y.; Cai, J.-Y., LASSO variable selection in data envelopment analysis with small datasets. *Omega* **2020**, *91*, 102019.
- (39) O'Connor, N. J.; Jonayat, A. S. M.; Janik, M. J.; Senftle, T. P., Interaction trends between single metal atoms and oxide supports identified with density functional theory and statistical learning. *Nature Catalysis* **2018**, *1*, 531-539.
- (40) Chen, Y.; Yu, G.; Chen, W.; Liu, Y.; Li, G.-D.; Zhu, P.; Tao, Q.; Li, Q.; Liu, J.; Shen, X., Highly active, nonprecious electrocatalyst comprising borophene subunits for the hydrogen evolution reaction. *Journal of the American Chemical Society* **2017**, *139*, 12370-12373.
- (41) Tedstone, A. A.; Lewis, D. J.; O'Brien, P., Synthesis, Properties, and Applications of Transition Metal-doped Layered Transition Metal Dichalcogenides. *Chemistry of Materials* **2016**, 28, 1965-1974.

- (42) Li, H.; Wang, L.; Dai, Y.; Pu, Z.; Lao, Z.; Chen, Y.; Wang, M.; Zheng, X.; Zhu, J.; Zhang, W., Synergetic interaction between neighbouring platinum monomers in CO₂ hydrogenation. *Nature nanotechnology* **2018**, *13*, 411.
- (43) Liu, G.; Robertson, A. W.; Li, M. M.-J.; Kuo, W. C.; Darby, M. T.; Muhieddine, M. H.; Lin, Y.-C.; Suenaga, K.; Stamatakis, M.; Warner, J. H., MoS₂ Monolayer Catalyst Doped with Isolated Co Atoms for the Hydrodeoxygenation Reaction. *Nature chemistry* **2017**, *9*, 810.
- (44) Zhao, J.; Zhao, J.; Cai, Q., Single transition metal atom embedded into a MoS₂ nanosheet as a promising catalyst for electrochemical ammonia synthesis. *Physical Chemistry Chemical Physics* **2018**, *20*, 9248-9255.
- (45) Wehling, T.; Lichtenstein, A.; Katsnelson, M., Transition-metal adatoms on graphene: Influence of local Coulomb interactions on chemical bonding and magnetic moments. *Physical Review B* **2011**, *84*, 235110.
- (46) Anisimov, V. I.; Aryasetiawan, F.; Lichtenstein, A., First-principles calculations of the electronic structure and spectra of strongly correlated systems: the LDA+ U method. *Journal of Physics: Condensed Matter* **1997**, *9*, 767.
- (47) Chen, Z.; Zhao, J.; Cabrera, C. R.; Chen, Z., Computational Screening of Efficient Single Atom Catalysts Based on Graphitic Carbon Nitride (g C_3N_4) for Nitrogen Electroreduction. *Small Methods* **2018**, 1800368.
- (48) Montoya, J. H.; Tsai, C.; Vojvodic, A.; Nørskov, J. K., The challenge of electrochemical ammonia synthesis: A new perspective on the role of nitrogen scaling relations. *ChemSusChem* **2015**, *8*, 2180-2186.
- (49) Zhang, L.; Sharada, S. M.; Singh, A. R.; Rohr, B. A.; Su, Y.; Qiao, L.; Nørskov, J. K., A theoretical study of the effect of a non-aqueous proton donor on electrochemical ammonia synthesis. *Physical Chemistry Chemical Physics* **2018**, *20*, 4982-4989.
- (50) Wang, P.; Kumar, R.; Sankaran, E. M.; Qi, X.; Zhang, X.; Popov, D.; Cornelius, A. L.; Li, B.; Zhao, Y.; Wang, L., Vanadium diboride (VB2) synthesized at high pressure: elastic, mechanical, electronic, and magnetic properties and thermal stability. *Inorg Chem* **2018**, *57*, 1096-1105.
- (51) Ling, C.; Niu, X.; Li, Q.; Du, A.; Wang, J., Metal-free single atom catalyst for N2 fixation driven by visible light. *Journal of the American Chemical Society* **2018**, *140*, 14161-14168.
- (52) Ji, S.; Wang, Z.; Zhao, J., A boron-interstitial doped C₂N layer as a metal-free electrocatalyst for N₂ fixation: a computational study. *J Mater Chem A* **2019**, 7, 2392-2399.
- (53) Xu, H.; Cheng, D.; Cao, D.; Zeng, X. C., A universal principle for a rational design of single-atom electrocatalysts. *Nature Catal* **2018**, *1*, 339-348.
- (54) De, S.; Bartók, A. P.; Csányi, G.; Ceriotti, M., Comparing molecules and solids across structural and alchemical space. *Physical Chemistry Chemical Physics Pccp* **2016**, *18*, 13754-13769.
- (55) Hou, Z.-Y.; Dai, Q.; Wu, X.-Q.; Chen, G.-T., Artificial neural network aided design of catalyst for propane ammoxidation. *Applied Catalysis A: General* **1997**, *161*, 183-190.